10.6 MICROMETER DETECTOR ARRAY

R. A. Lange, et al

AIL
Deer Park, New York

December 1972

10.6 MICROMETER DETECTOR ARRAY

Semiannual Report with Quarterly Technical Status Report
(1 August 1972 to 1 November 1972)

December 1972

by

R. A. Lange, J. Wolczok, and D. Yustein

AIL Report 0123-I-2
Prepared Under Contract N00014-72-C-0446
Project Code 2E90K21

for

Office of Naval Research
Washington, D. C.

Sponsored by

Advanced Research Projects Agency
ARPA Order No. 1806, Amendment No. 2/02-09-72

by

AIL, a division of Cutler-Hammer
Deer Park, New York 11729

DOCUMENT CONTROL DATA - R & D

(Security classification of title, body of abstract and indexing annotation must be entered when the overall report is classified)

1. ORIGINATING ACTIVITY *(Corporate author)*
AIL, a division of Cutler-Hammer
Deer Park, New York 11729

2a. REPORT SECURITY CLASSIFICATION
Unclassified

2b. GROUP

3. REPORT TITLE
10.6 MICROMETER DETECTOR ARRAY

4. DESCRIPTIVE NOTES *(Type of report and inclusive dates)* Semiannual Report with Quarterly Technical Status Report (1 August 1972 to 1 November 1972)

5. AUTHOR(S) *(First name, middle initial, last name)*
R. Lange, J. Wolczok, and D. Yustein

6. REPORT DATE	7a. TOTAL NO. OF PAGES	7b. NO. OF REFS
December 1972	28	4

8a. CONTRACT OR GRANT NO	9a. ORIGINATOR'S REPORT NUMBER(S)
N00014-72-C-0446	0123-I-2
b. PROJECT NO. ZE90K21	
c.	9b. OTHER REPORT NO(S) *(Any other numbers that may be assigned this report)*
d.	

10. DISTRIBUTION STATEMENT will follow.

11. SUPPLEMENTARY NOTES	12. SPONSORING MILITARY ACTIVITY
	Office of Naval Research Washington, D.C.

13. ABSTRACT

Analyses were performed on various aspects of the multielement heterodyne technology including high density cabling techniques, image plane dissection to provide 10 × 10 (100 element) spatial elements, heating effects in a matrix array, and 4 K cooler requirements to obtain the desired system sensitivity.

Measurements were carried out on HgCdTe photodiodes that showed cutoff frequencies of greater than 200 MHz and a maximum noise equivalent power (NEP) of 1.7×10^{-19} W/Hz over the 200 MHz bandwidth.

14 KEY WORDS	LINK A		LINK B		LINK C	
	ROLE	WT	ROLE	WT	ROLE	WT
Heterodyne Imaging Array						
PV - HgCdTe Photomixers						
Array Image Dissector						

10.6 MICROMETER DETECTOR ARRAY

Semiannual Report with Quarterly Technical Status Report
(1 August 1972 to 1 November 1972)

December 1972

by

R. A. Lange, J. Wolczok, and D. Yustein

AIL Report 0123-I-2
Prepared Under Contract N00014-72-C-0446
Project Code 2E90K21

Date of Contract:	1 April 1972
Expiration of Contract:	31 December 1972
Amount of Contract:	$113,211

for

Office of Naval Research
Washington, D.C.

Sponsored by

Advanced Research Projects Agency
ARPA Order No. 1806, Amendment No. 2/02-09-72

by

AIL, a division of Cutler-Hammer
Deer Park, New York 11729

TABLE OF CONTENTS

LIST OF ILLUSTRATIONS

I. INTRODUCTION AND QUARTERLY TECHNICAL SUMMARY

This is the first Semiannual Technical Report under Contract N00014-72-C-0446, having as its objective the development of a technology required to build a large array of high-speed heterodyne receivers for 10.6-micrometer laser radiation. Toward this end the following areas will be examined:

- High density cabling techniques aimed at obtaining low electrical crosstalk between elements, low thermal conductivity, and low electrical loss
- Thermal analysis of matrix arrays which operate at 77 and 4.2 K and provide either 150 or 1500 MHz instantaneous response
- Thermal mockup of cabling techniques for cryogenically cooled (77 K), wide IF band (1500 MHz) array
- Image plane dissection techniques using batch processing techniques for an array of 100 elements or larger
- Optical evaluation of four HgCdTe photodiodes on a subassembly of the matrix array design used for the thermal mockup.

The following tasks have been covered during this report period with the following results or conclusions:

- An analysis of high density cabling techniques has been carried out and the results indicate that a 0.034 inch diameter stainless steel, semirigid cable is a good engineering choice to meet the simultaneous requirements of low loss, low crosstalk, and low thermal conductivity.
- Image plane dissection techniques are being investigated with the goal of batch processing the final image dissector. Some of the techniques have been breadboarded, however, the optimum technique has not yet been chosen.
- Thermal analyses of detector mounts and a prediction of system sensitivity based upon thermal loading were performed and provided sufficient information to allow prediction of system performance when used with a 4.2 K, limited capacity, closed cycle cooler.

II. HIGH DENSITY CABLING TECHNIQUES

High density cabling techniques were investigated in order to determine the thermal load, electrical loss, and crosstalk for two types of cables which might be suitable for connecting the cryogenically cooled photomixers and the ambient temperature IF preamplifiers. Tests were conducted wherever practical to check the analytical results. The analysis was done for a 50-ohm twin lead cable and a 50-ohm semirigid coaxial cable. The twin lead cable consisted of stainless steel conductors 0.010 inch in diameter separated by a polyurethane spacer of 0.015 inch. The coaxial line was semirigid with a solid outer sheath of stainless steel (0.034-inch in diameter) and a center conductor of copper weld material (0.008 inch in diameter).

A comparison of the thermal conduction for the two cables is given in Figure 1, using two mixer temperatures (4.2 and 77 K). The amount of heat transferred from the external environment (300 K) through the cable to the photomixer (77 K) is seen to decrease asymptotically toward zero as the cable lengths are increased. The advantage of a twin lead can be seen to diminish as greater cable lengths are required. Observing in Figure 1A, for 10 centimeters of cable length, the twin lead transfers 10.2 milliwatts of heat, compared to 28.5 milliwatts for the coaxial cable, while at 20 centimeters, the twin lead transfers 5 milliwatts and the coaxial cable transfers 14.5 milliwatts. While the ratio of the heat load between the two types of cables remains constant, the difference in the absolute amount of heat transferred was cut in half by increasing the cable length from 10 to 20 centimeters. Similar results are obtained from Figure 1B for the 4.2 K photomixers.

The variation of electrical loss with cable length are given in Figure 2 for a nitrogen-cooled photomixer and IF frequencies of 150 and 1500 MHz. The coaxial line is seen to have a definite advantage of providing lower electrical loss for the particular transmission lines considered between 300 and 77 K. Measurements were carried out on the electrical loss of the 50-ohm coaxial cable and the measurement results are compared to the calculated values in Table 1.

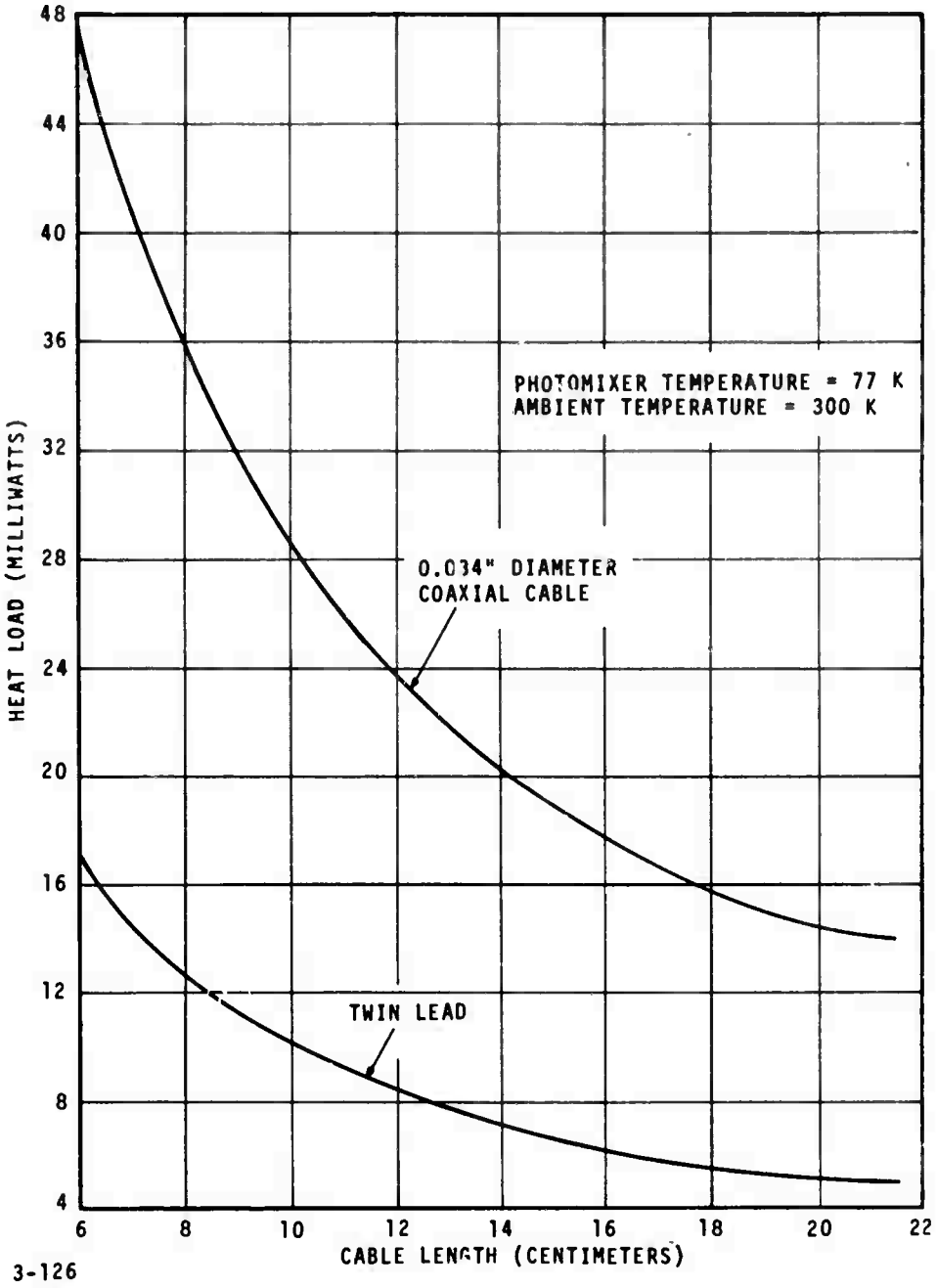

FIGURE 1. CALCULATED HEAT LOAD VERSUS CABLE LENGTH FOR COAXIAL AND TWIN LEAD CABLES (SHEET 1 OF 2)

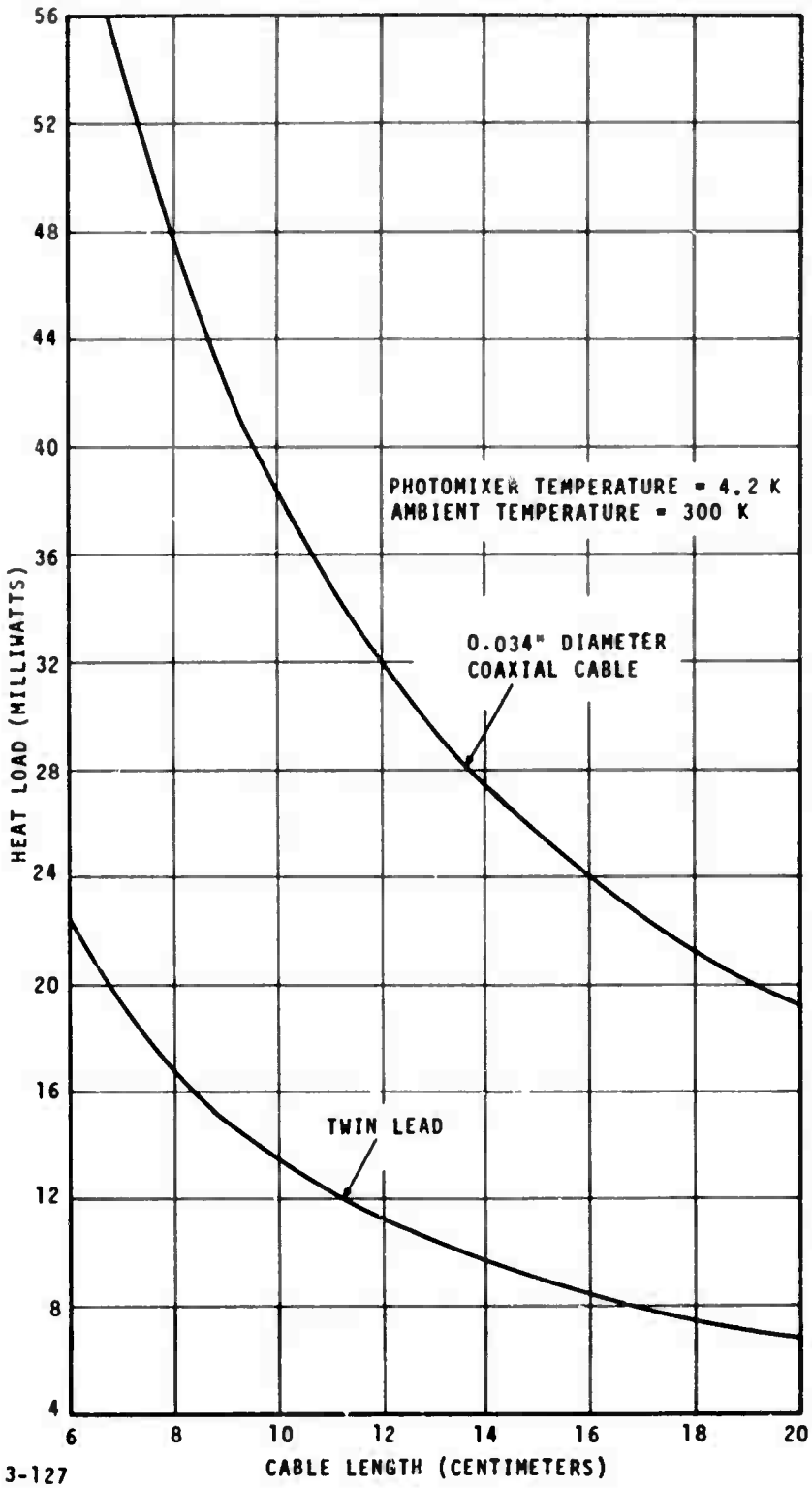

FIGURE 1. CALCULATED HEAT LOAD VERSUS CABLE LENGTH FOR COAXIAL AND TWIN LEAD CABLES (SHEET 2 OF 2)

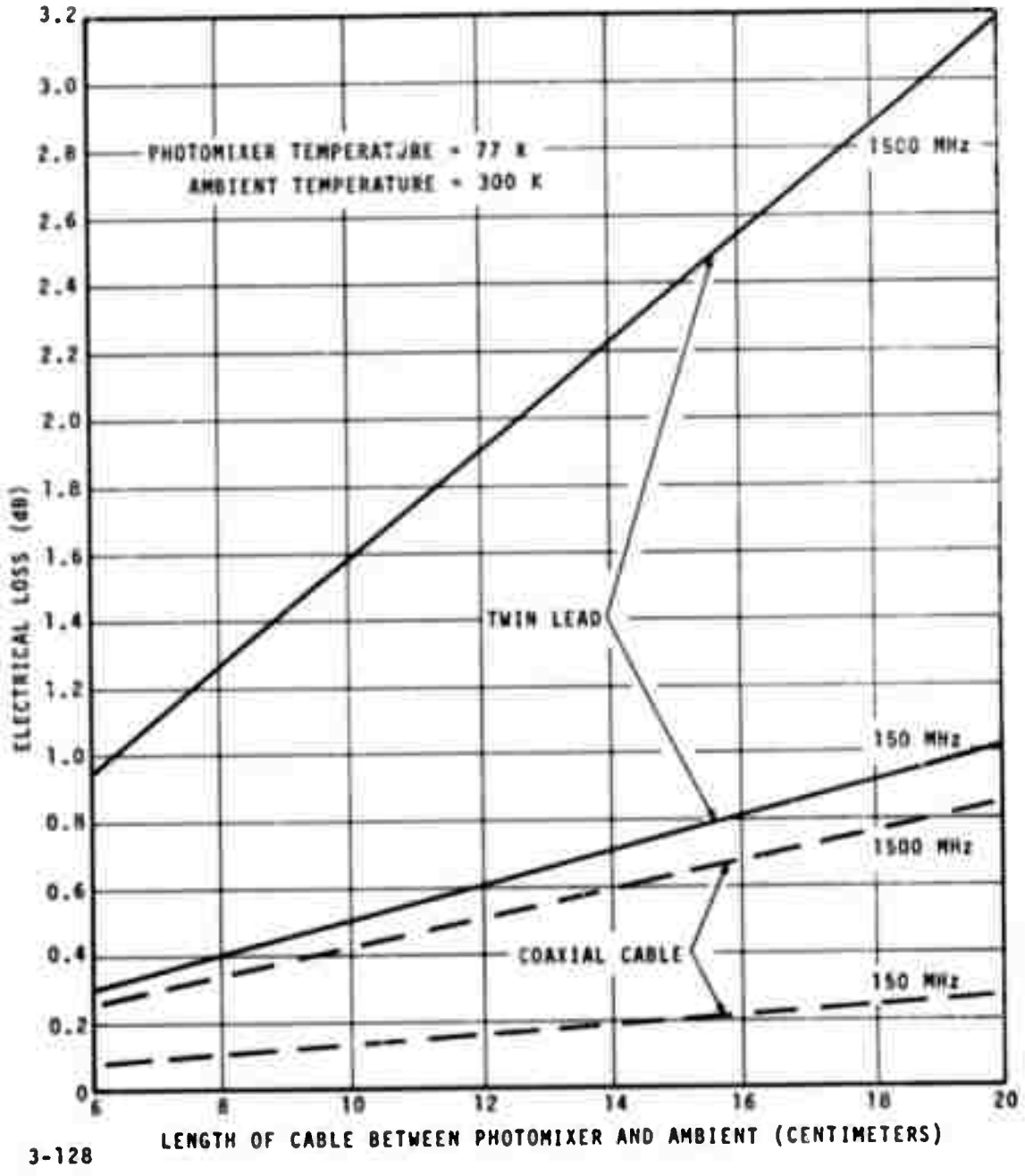

FIGURE 2. CALCULATED ELECTRICAL LOSS VERSUS CABLE LENGTH FOR COAXIAL AND TWIN LEAD CABLES

TABLE 1. MEASURED AND CALCULATED ELECTRICAL LOSS OF A 12-FOOT LENGTH OF 50-OHM COAXIAL CABLE*

IF Frequency (MHz)	Electrical Loss			
	Calculated (77 to 300 K)		Measured (300 K)	
	(dB)	(dB/ft)	(dB)	(dB/ft)
150	4.86	0.405	6	0.5
1000	-	-	15	1.25
1500	15.5	1.29	19	1.58

At an IF frequency of 1500 MHz, the measured loss was 1.58 dB/ft compared to the calculated value of 1.29 dB/ft. Similarly for an IF of 150 MHz, the measured signal attenuation was 0.5 dB/ft and the calculated value was 0.40 dB/ft. The discrepancy can, in part, be attributed to an approximation made in the calculations whereby it was assumed that the center conductor was composed entirely of copper. In actuality, part of its center core contained a layer of stainless steel. Since the resistivity of copper is lower than steel, the calculated loss will be accordingly lower. In addition, the measured loss was for a 300 K coaxial cable not having the benefit of one end cooled to 77 K which reduced the average loss per unit length.

An analysis of the crosstalk between twin leads was performed for the worst case condition where the two lengths of cross-coupling cables were a quarter wavelength long at the particular IF frequency. The resultant crosstalk for cables separated by twice the conductor spacing was -11.5 dB for the 50-ohm twin lead cable and -13 dB for the 300-ohm twin lead line. The resultant crosstalk measured for the 300-ohm twin lead cable was -15 dB which was in agreement with the calculated value of -13 dB for cables separated by the same spacing.

For the case of a liquid nitrogen-cooled photomixer and an IF frequency of 1500 MHz, it can be seen that the 50-ohm coaxial line has definite advantages over a twin lead line. A coaxial cable length of 15 centimeters results in a calculated electrical loss of only 0.63 dB, compared to

*The stainless steel outer conductor has a diameter of 0.034 inch and a thickness of 0.003 inch. The copper weld inner conductor has a diameter of 0.008 inch.

2.4 dB for a twin lead line, and a crosstalk isolation of approximately -100 dB, compared to about -15 dB for a twin lead line. These advantages more than compensate for the disadvantage of the higher heat load (19 milliwatts) of the coaxial line. Based on these considerations, the coaxial cabling has been chosen for the 77 K 1500 MHz response heterodyne array.

III. IMAGE PLANE DISSECTION TECHNIQUES

Image plane dissection techniques are being investigated toward a goal of batch processing the elements for arrays of 100 elements or larger. Five techniques are presently under study with preliminary fabrication and testing being conducted where possible within the scope of the present program. The five approaches are:

- Fresnel lens array prepared by a cold forming technique
- Molding of GeSbSe IR transmitting glass
- Fresnel zone plate arrays
- Batch processing of germanium lenses
- Photolithographic fabrication of thin film lens arrays.

A. FRESNEL LENS ARRAY

A Fresnel lens is being constructed for use at 10 micrometers to test the feasibility of cold forming techniques. Previous technology in this area has been confined to the visible and near infrared due to a lack of suitable materials transmitting in the infrared at 10.6 micrometers. A material (silver bromide) has been identified which appears likely to fit the needs of the array transmission at 10.6 micrometers. The material has the ability to cold flow which is necessary for the fabrication technique employed, however it is photosensitive, changing its transmission if exposed to ultraviolet light for extended periods of time. This does not present a restriction to the array application since the lenses will be located in a dewar flask behind a germanium window. The germanium does not pass the ultraviolet so that no deterioration of the lens is likely to result.

B. MOLDING OF IR GLASS

The molding of a GeSbSe glass array has been investigated and appears to be feasible. However, no array will be fabricated due to the unavailability of a suitable source having sufficient experience in modling this glass. The scope of the present program is such that a subcontract to explore this technique is not called for at this time.

The material's transmission is 65 percent (1 to 11 micrometers) with virtually all of the loss due to reflection and minimum material absorption up to 11 micrometers (reference 1). Antireflection coatings are available which increase the transmission in the 8 to 11 micrometer band to better than 90 percent. This material has been readily formed into various shapes by melt-casting with high quality lenses resulting. Consultations with the glass manufacturers indicate that the molding of a multiple lens array as a single unit is feasible and the tolerances will be set by the master mold which can be very precisely controlled.

C. FRESNEL ZONE PLATE ARRAYS

Fresnel zone plate arrays can also be used for the image-dissection technique with fabrication techniques well within the state of the art. They, however, have the disadvantage of a high optical loss of the signal energy (3 dB) due to reflection of the energy from alternate out-of-phase zones. It is felt that this loss cannot be tolerated in a high sensitivity receiver.

D. BATCH PROCESSING OF Ge LENSES

The batch processing of individual square germanium lenses can be accomplished with sufficient tolerances to ensure a minimum buildup of dimensional tolerances across the array. However, the area of potential difficulty in using this approach is the control of the center-to-center spacing of the focused spots in the focal plane. Any cocking of the lens or shift in optical axis from the lens center will shift the position of the focused spot off the desired optical axes of the array.

E. PHOTOLITHOGRAPHIC FABRICATION OF LENSES

Photolithographic techniques for the fabrication of a thin film lens array have come about as a result of the utilization of integrated circuit technology. The lens profile is approximated by an N-step phase quantization with the layers formed by successive photo-engravings using N masks (reference 2). Experimental results by d'Auria and others show

---

[1] Patterson, R. J., "A GeSbSe Infrared Transmitting Glass," Proceedings of IRIS, Vol II, No. 1, October 1966.

[2] d'Auria, L., Huignard, J. P., Roy, A. M., Spitz, E., "Photolithographic Fabrication of Thin Film Lenses," Optics Communications, Vol 5, No. 4, p 232, July 1972.

a 63 percent diffraction of the incident energy into the main focus of the lens for a four -level lens as compared with the theoretical 81 percent. This resultant 63 percent efficiency is judged to be below that already feasible using several of the techniques described previously.

Based upon the data available to this point, we must conclude that the relatively low efficiency yielded by the Fresnel zone plate arrays and the photolithographic thin film lenses make them impractical for a near quantum noise-limited array.

IV. 4.2 K COOLER REQUIREMENTS FOR A 100-ELEMENT GERMANIUM ARRAY

A matrix array design for Ge:Cu(Sb) heterodyne mixer elements has been developed under a previous program, N00014-68-C-0273, entitled "Advanced Capability Infrared Receiver System." This program developed a high frequency array structure capable of employing heterodyne mixer elements in a 10 × 10 configuration. This design was implemented on a smaller scale in a subsequent program, N00014-70-C-0407, where a 2 × 2 array was built incorporating a microwave integrated circuit impedance matching network to provide the optimum high frequency performance. Based upon the array performance measured during this program, we can predict with reasonable certainty the receiver sensitivity as a function of the dc bias and local oscillator power dissipated in the mixer element.

Figure 3 shows the predicted system NEP's at 150 and 1500 MHz for a single channel of an array including the optics losses, mixer quantum efficiency, impedance matching network, and second stage noise contributions due to the preamplifier and associated signal processing electronics. The individual mixer impedances are approximately 1000 ohms with the application of 50 milliwatts of 10.6 local oscillator power. From this we can see that a total of 200 milliwatts (150 milliwatts dc bias plus 50 milliwatts local oscillator) is required per array element in order to obtain a sensitivity of 2.2×10^{-19} W/Hz at an IF frequency of 1500 MHz. Significant decreases in the dissipated power can be obtained to more reasonably meet the present capabilities of coolers at 4.2 K providing that the system sensitivity can be degraded slightly. As an example, the thermal requirements can be reduced to 100 milliwatts per array element if the total system is capable of operating with its overall system sensitivity of 4.7×10^{-19} W/Hz at the highest IF frequency (1500 MHz).

If the bandwidth requirement of the system is only 150 MHz, which would adequately provide for a signal from a moving aircraft, the overall system sensitivities can be improved to 1.55 and 2.7×10^{-19} W/Hz, for total (LO and dc) bias powers of 200 and 100 milliwatts, respectively.

A system which was designed to operate over a 150 MHz bandwidth could be expected to produce system NEP's which are a factor of two more than the wideband system data for 150 MHz shown in Figure 3 and would require less local oscillator power.

Using the appropriate approximations, overall system sensitivities of 1.1×10^{-19} and 2.2×10^{-19} W/Hz are predicted for total power dissipations of 100 and 50 milliwatts, respectively. These results are summarized in Table 2 which gives the expected sensitivity per channel of a 10×10 array with the LO and dc bias thermal load.

TABLE 2. PREDICTED SYSTEM PERFORMANCE USING A COPPER DOPED GERMANIUM PHOTOMIXER

System Bandwidth	System Sensitivity Per Channel	4.2 K Array Cooler Requirements
1500 MHz	2.2×10^{-19} W/Hz	20 watts
1500 MHz	4.7×10^{-19} W/Hz	10 watts
150 MHz	1.1×10^{-19} W/Hz	10 watts
150 MHz	2.2×10^{-19} W/Hz	5 watts

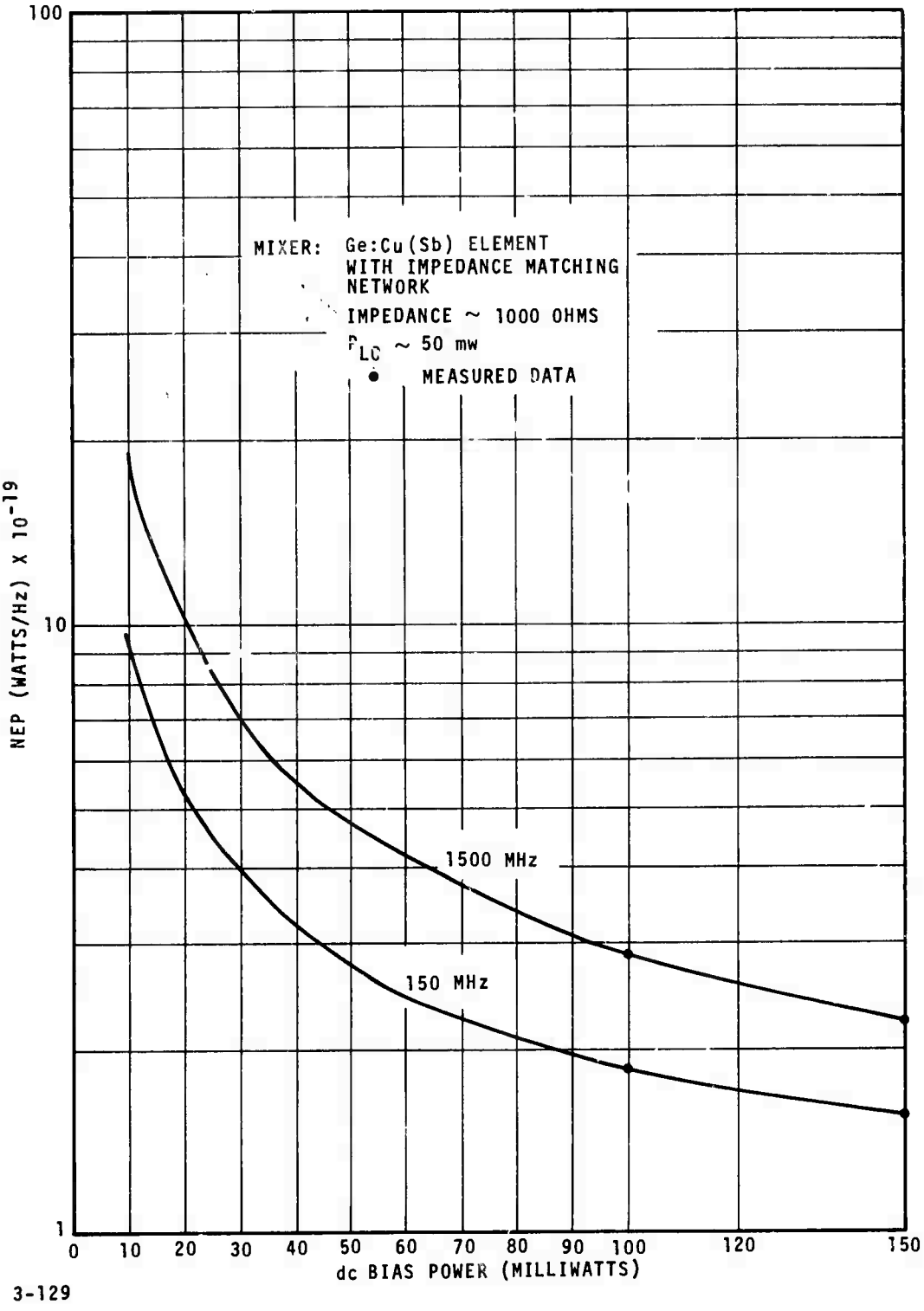

FIGURE 3. PREDICTED NEP VERSUS DC BIAS POWER FOR A TYPICAL WIDEBAND Ge:Cu(Sb) RECEIVER AT 10.6 MICROMETERS

V. THERMAL ANALYSIS OF PHOTOMIXER ARRAY MOUNTS

A. DETERMINATION OF THE TEMPERATURE RISE OF A 10 × 10 PHOTOMIXER ARRAY

The temperature at the surface of the detector (Figure 4) is calculated for the steady state case by starting with the thermal resistances between the mixer with its LO and dc bias power loads and the 77 K liquid nitrogen cold sink. From Fourier's expression for heat conduction, the thermal resistance of a material is determined by the distance the heat must travel through the material divided by the cross-sectional area times a constant for the material (thermal conductivity). The thermal resistances for the various portions of the heat sink are 0.55 K/W for the BeO substrate, 1.3 K/W for the copper, and 25 K/W for the KMER adhesive between the mixer, substrate, and copper base. The temperature difference between mixer and cold sink is obtained from equation 1:

$$\Delta T = \sum Q R_{Th} \tag{1}$$

For an assumed 2 milliwatts of input heat load due to the incident laser LO and thermal resistance of 26.8 K/W, a ΔT or temperature rise of 0.054 K above the heat sink can be anticipated for the fully illuminated PV-HgCdTe mixer operating at 77 K. As a result of this very small temperature rise of the photomixer, we can conclude that there will be no deterioration of the sensitivities of the central mixer elements of a 77 K PV-HgCdTe photomixer matrix array.

B. DETERMINATION OF THE TEMPERATURE RISE AT THE CENTER OF 10 × 10 Ge PHOTOMIXER ARRAY

As in the preceding analysis, the temperature differential at a point can be determined by the sum of the thermal resistance between the point in question and the heat sink multiplied by the heat load applied. In the case of the 10 × 10 element mixer array surrounded by a 4.2 K heat sink, we assume a temperature maximum to occur at the center of the array. In setting up our model of the heat flow for this array, the following assumption is made: because of the imperfect interfaces between the rows of the array, the primary heat flow will occur along the horizontal direction for

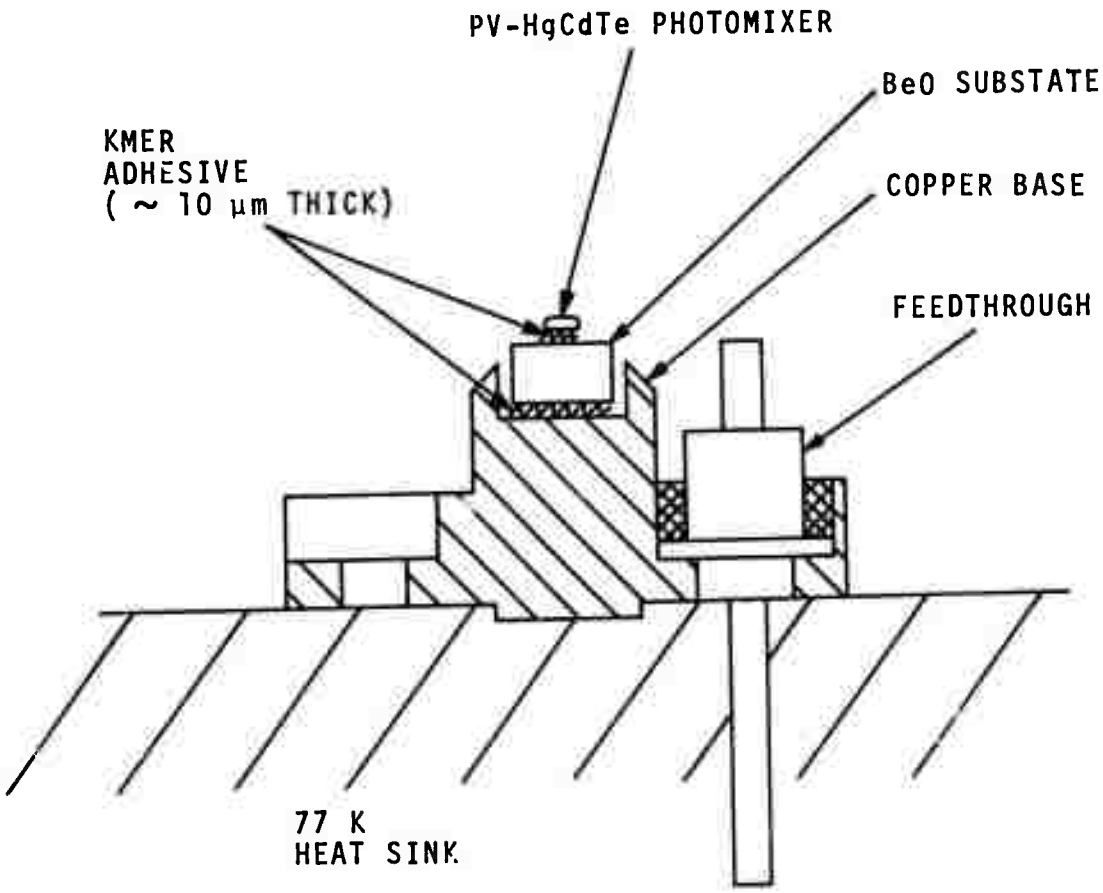

FIGURE 4. DETECTOR MOUNT FOR 77 K PV-HgCdTe PHOTOMIXER

each individual layer of detectors. A single row of the detector array is represented by the thermal resistances in Figure 5. The heat input to each detector is represented by Q. Because of symmetry with respect to the center of the row, only half the row need be considered. The temperature developed at the most interior detector is calculated from thermal resistances $R_a = 0.37$ K/W and $R_b = 1.3$ K/W with thermal loads (LO and dc bias) of 150 milliwatts per detector. The sum of the temperature differentials from point 1 to point 8 (heat sink at 4.2 K) results in a temperature rise of 6.8 K at this interior detector. The absolute temperature at this point then reaches 11 K in the steady state case.

The temperature rise to 11 K of an antimony-compensated germanium photomixer is expected to degrade the frequency response but not sensitivity level below the cutoff frequency of the mixer element. We can estimate this degradation in frequency response and sensitivity degradation from reference 3 which shows a plot of response time (τ) as a function of applied electric field for a compensated germanium photomixer at 5 and 21 K. The response time degradation over the 16 K temperature interval is approximately $1.35\ \tau_{5\ K}$. Approximating the temperature dependence, we calculate a behavior of $\tau \sim T^{0.2}$ so that the response time degradation will be on the order of $1.17\ \tau_{5\ K}$ with a corresponding 15 percent lowering of the cutoff frequency.

Reference 3 also contains a plot of carrier mobility as a function of temperature for a partially compensated germanium detector. From 5 to 11 K, the degradation of mobility was observed to be approximately 15 percent. From equations 2 and 3 for mixer conversion gain (G) and (NEP), we get:

$$G = \frac{\eta q \mu \tau}{2h\nu_2 (1 + \omega^2 \tau^2)} \left(\frac{V}{L}^2 \right) \tag{2}$$

$$NEP = \underbrace{\frac{2\ h\nu_s B}{\eta}}_{\text{quantum noise term}} + \underbrace{\frac{K (T_m + T'_{IF})\ B}{G}}_{\text{degradation from quantum noise limit term}} \tag{3}$$

[3] Buczek, C., and Picus, G.S., "Applied Physics Letters 11," p 125, 1967.

where

μ = carrier mobility

τ = mixer time constant

We can see that τ enters the gain expression in two places. The first is the frequency response which affects the gain as $1/(1 + \omega^2 \tau^2)$. The second is the $(\mu\tau)$ product which affects the conversion gain at all frequencies. From this we can conclude that to a first approximation, the gain is unaffected below the cutoff frequency since the mobility decreases by ~15 percent and the time constant increases by ~15 percent leaving the $\mu\tau$ product approximately unchanged.

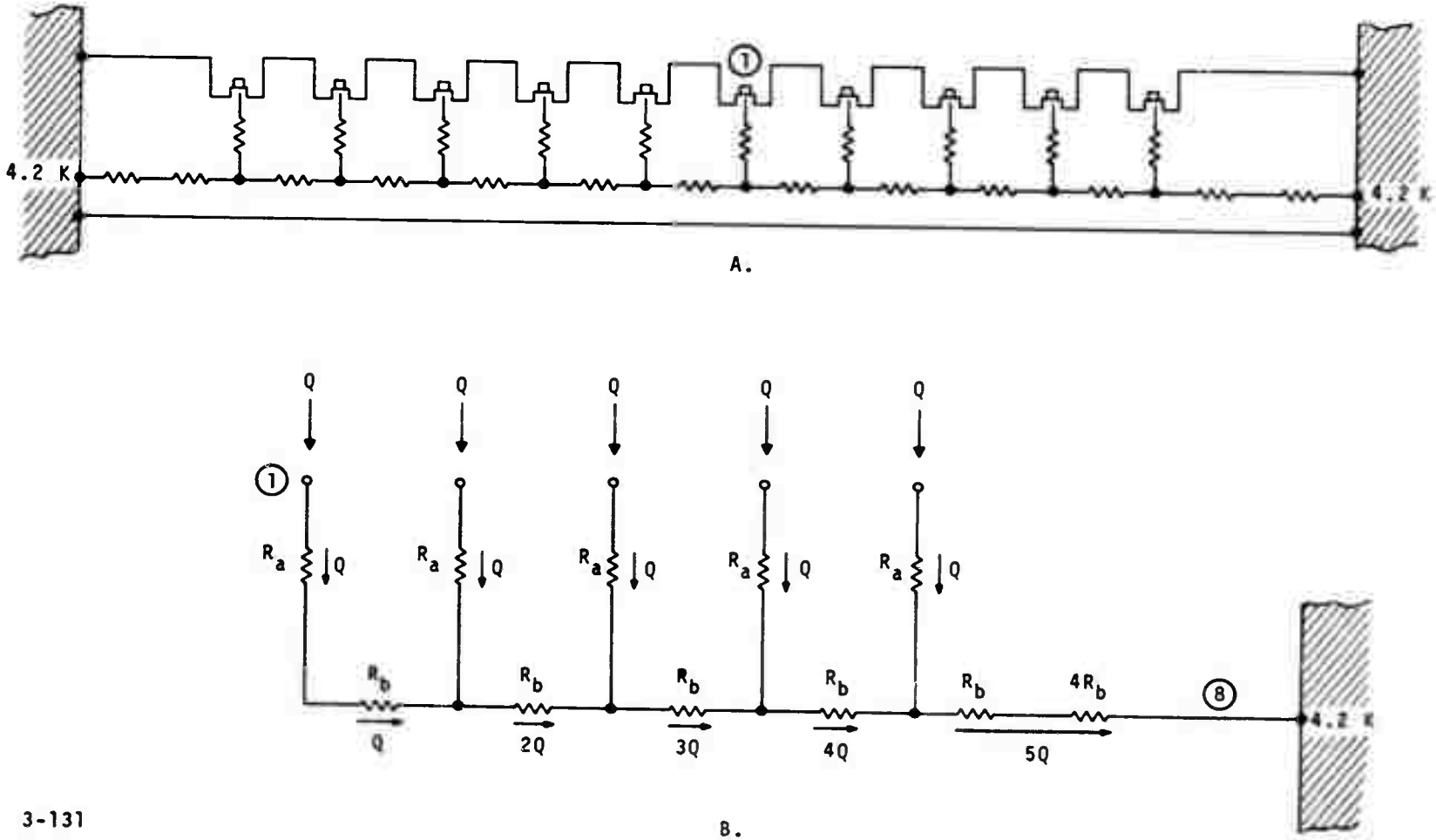

FIGURE 5. DETECTOR MODULE FOR A 4.2K GERMANIUM DOPED PHOTOMIXER ARRAY OF 100 ELEMENTS (10 BY 10 CONFIGURATION)

VI. BREADBOARD ARRAY OF HgCdTe PHOTODIODES

A subassembly of the 10 × 10 element array structure for 1.5 GHz operation is being constructed to perform laboratory testing of the matrix array design. The array is being implemented using five HgCdTe photodiodes with frequency response approaching or exceeding 150 MHz. Two of the photodiodes have been received and laboratory measurements have been performed to determine such parameters as photomixer impedance, quantum efficiency, frequency response, and sensitivity (NEP). When the breadboard array is fully implemented with the five HgCdTe photodiodes, measurements will be made to ascertain how well matched the photomixers are for efficient array operation. At that time, all five mixers will be illuminated with a uniform LO field and the array patterns of the mixers will be matched varying both the mixer bias and the gain in each channel.

The measured small signal ac quantum efficienty at 10.6 micrometers for the two photomixers is given in Table 3.

TABLE 3. MIXER AC QUANTUM EFFICIENCY FOR PV-HgCdTe PHOTOMIXERS AT 77 K

Mixer	Ac Quantum Efficiency	Mixer Bias Voltage	Photoinduced Current
A	38 percent	-0.2 volts	0.9 mA
	35 percent	-0.4 volts	0.8 mA
B	47 percent	-0.2 volts	1.12 mA
	47 percent	-0.4 volts	0.8 mA

The measurement was performed with the mixer fully illuminated by local oscillator power to obtain a more precise indication of the quantum efficiency in the mixing mode. Both of the measured photomixers have high quantum efficiencies in the 35 and 47 percent range.

Frequency response and sensitivity measurements were then performed using the combination of a direct NEP measurement at 20 MHz

and the indirect noise measurement technique (reference 4) for frequency response. The direct NEP was obtained using a CO_2 heterodyne setup with a fixed frequency offset of 20 MHz. The indirect noise measurement technique measures the ratio of the photoinduced shot noise from the diode to the thermal noise level of the IF preamplifier. The IF amplifier used to evaluate the photomixers was extremely wideband with a frequency response of 10 to 1500 MHz and a noise factor of approximately 5 dB. The directly measured NEP's are presented in Table 4.

Table 4. MIXER NEP AT 20 MHz FOR TWO PV-HgCdTe PHOTOMIXERS AT 77 K

Mixer No.	NEP at 20 MHz	Mixer Bias Voltage	Photoinduced Current
A	9.9×10^{-20} W/Hz	-0.2 volts	0.83 mA
	1.34×10^{-19} W/ Hz	-0.8 volts	0.48 mA
B	1.65×10^{-19} W/Hz	-0.2 volts	1.04 mA
	1.84×10^{-19} W/ Hz	-0.4 volts	1.26 mA

The variation of NEP with photoinduced current for mixer A is shown in Figure 6. From this curve the variation of NEP with photoinduced current can be seen with the NEP asymptotically approaching the quantum noise limit.

With the NEP at 20 MHz established, the ratio of P_{shot}/P thermal was then measured from 20 to 700 MHz. This data is shown in Figure 7. The breakpoint frequency of the photomixer, as determined from these curves, is 220 MHz for mixer A and 205 MHz for mixer B.

---

[4] Arams, F. R., Sard, E. W., Peyton, B. J., and Pace, F. P., "Infrared Heterodyne Detection with Gigahertz IF Capability," IEEE Journal of Quantum Electronics, Vol. QE-3, No. 11, pp 484, November 1967.

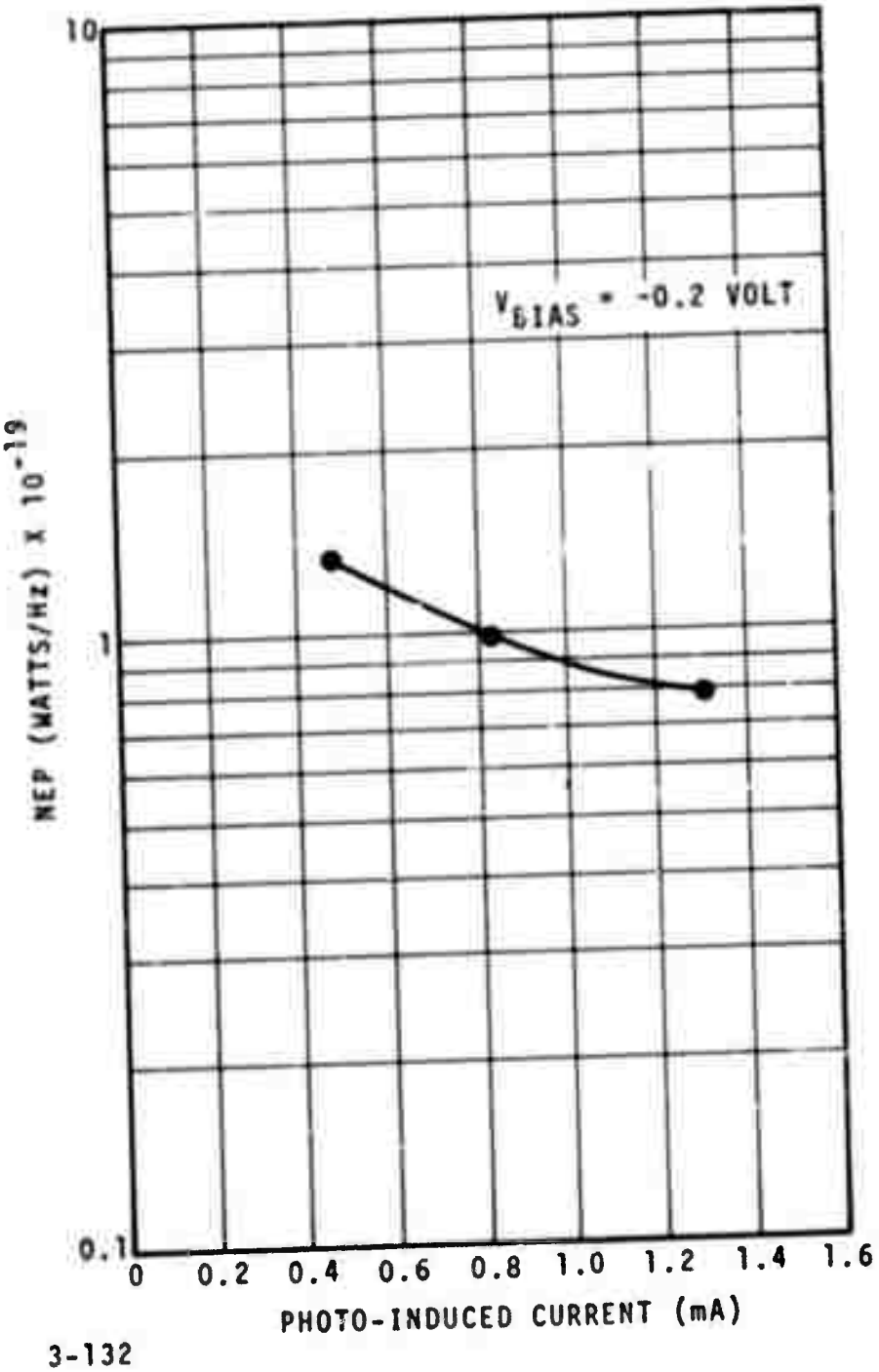

FIGURE 6. MEASURED NEP VARIATION OF MIXER A AS A FUNCTION OF PHOTO-INDUCED CURRENT

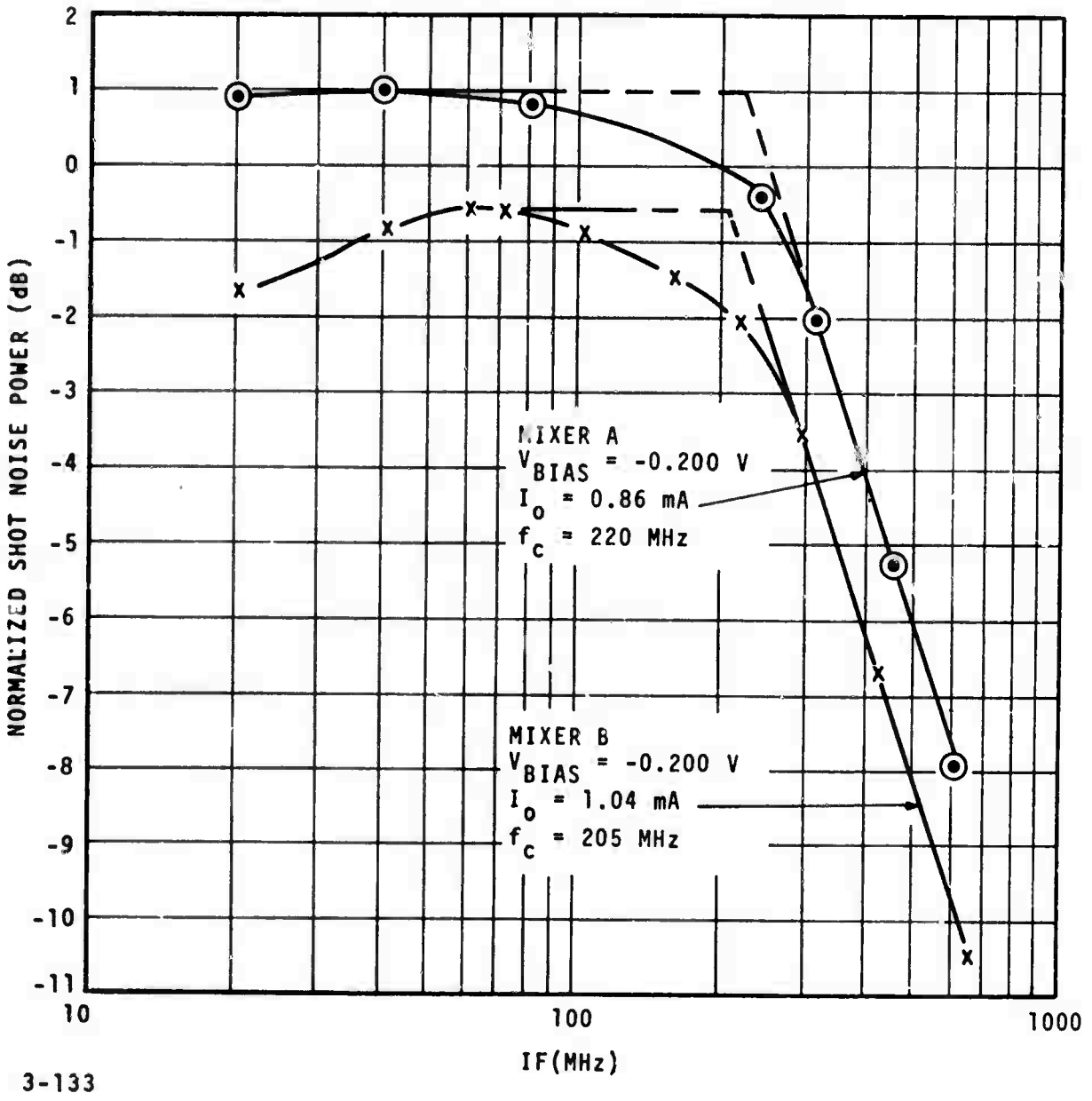

FIGURE 7. MEASURED VARIATION OF PHOTO-INDUCED SHOT NOISE AS A FUNCTION OF IF FREQUENCY

Combining the data from Table 4 and Figure 7, the variation in NEP with frequency can be inferred from equation 4.

$$NEP/_{P_{min}} = 1 + \frac{P_s}{P_{th}} \qquad (4)$$

The resulting NEP for the two mixers is shown in Figure 8. The measured NEP was less than 1.65×10^{-19} W/Hz from 20 to 150 MHz for both mixers, with A maintaining this sensitivity out to 400 MHz.

During the next report period, three more photomixers will be tested and a uniformity of response will be measured with the mixers operating as an array with a uniform local oscillator irradiating each mixer element.

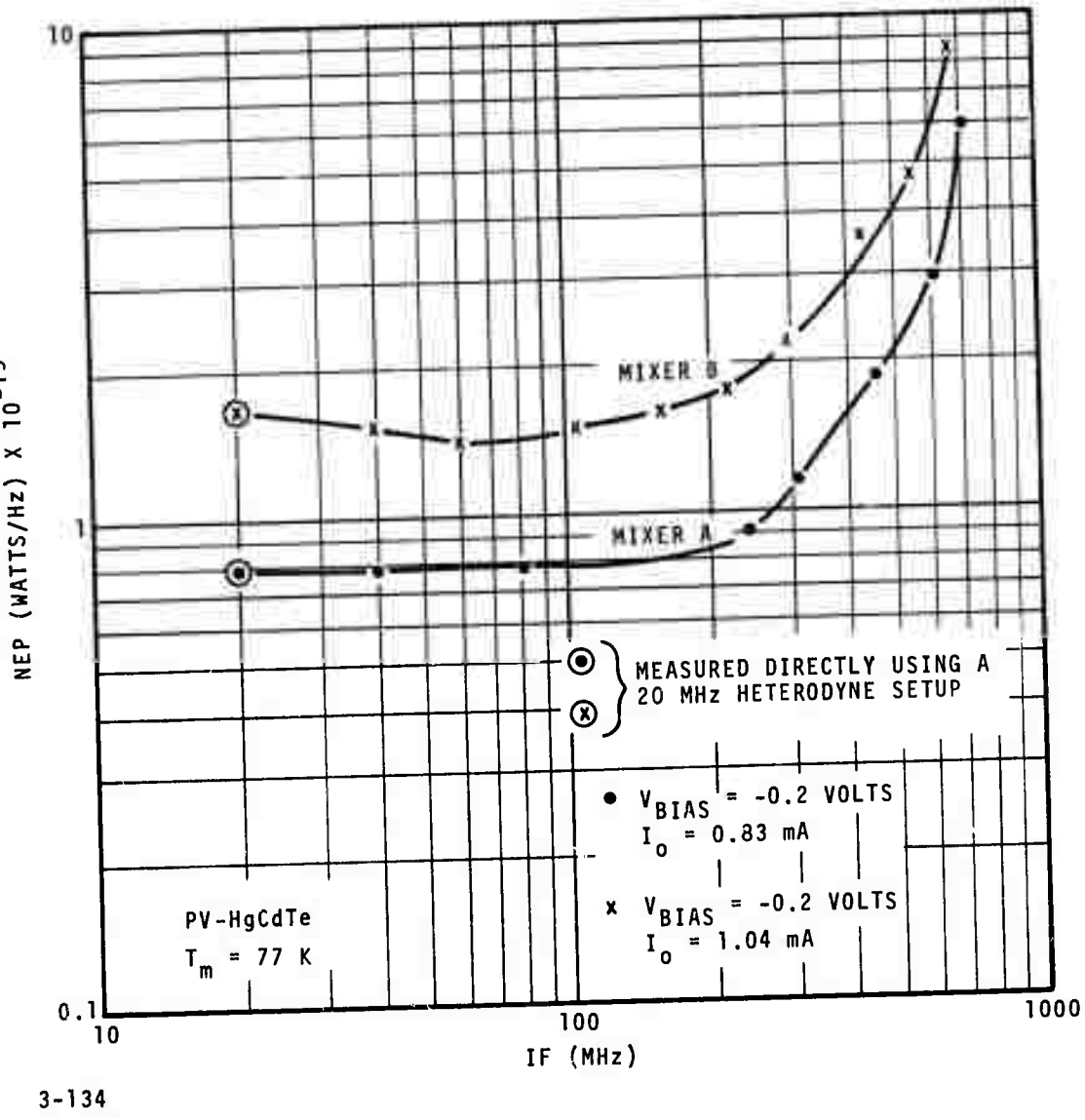

FIGURE 8. MEASURED RECEIVER NEP AS A FUNCTION OF IF FREQUENCY

VII. PLANS FOR NEXT QUARTER

- The thermal mockup of a 77 K, 1.5 GHz, 10 × 10 array will be completed and tested
- The remaining HgCdTe photodiodes will be tested and mounted onto a subassembly of the matrix array design
- Array uniformity and electrical crosstalk measurements will be carried out using the five photodiodes in the subassembly
- Parametric tradeoffs will be performed to determine size, weight, optical requirements, and thermal requirements for a 77 K, 1.5 GHz, 10 × 10 array.